

Statistics of Green's functions on a disordered Cayley tree and the validity of forward scattering approximation.

P. A. Nosov¹ I. M. Khaymovich^{2,3*} A. Kudlis⁴ and V. E. Kravtsov^{5,6}

1 Stanford Institute for Theoretical Physics, Stanford University, Stanford, California 94305, USA

2 Max-Planck-Institut für Physik komplexer Systeme, Nöthnitzer Straße 38, 01187-Dresden, Germany

3 Institute for Physics of Microstructures, Russian Academy of Sciences, 603950 Nizhny Novgorod, GSP-105, Russia

4 Department of Physics and Engineering, ITMO University, St. Petersburg, 197101, Russia

5 Abdus Salam International Center for Theoretical Physics - Strada Costiera 11, 34151 Trieste, Italy

6 L. D. Landau Institute for Theoretical Physics - Chernogolovka, Russia

* ivan.khaymovich@gmail.com

March 1, 2022

Abstract

The accuracy of the forward scattering approximation for two-point Green's functions of the Anderson localization model on the Cayley tree is studied. A relationship between the moments of the Green's function and the largest eigenvalue of the linearized transfer-matrix equation is proved in the framework of the supersymmetric functional-integral method. The new large-disorder approximation for this eigenvalue is derived and its accuracy is established. Using this approximation the probability distribution of the two-point Green's function is found and compared with that in the forward scattering approximation (FSA). It is shown that FSA overestimates the role of resonances and thus the probability for the Green's function to be significantly larger than its typical value. The error of FSA increases with increasing the distance between points in a two-point Green's function.

Contents

| | | |
|----------|---|----------|
| 1 | Introduction | 2 |
| 2 | TM equation and renormalization of disorder distribution | 4 |
| 3 | Moments of real Green's functions | 6 |
| 3.1 | Integration over the phases | 7 |
| 3.2 | Integration over anti-commuting variables | 8 |
| 3.3 | Integration over s_k and \tilde{s}_k | 10 |
| 3.4 | Iterative representation of the result | 12 |

| | | |
|----------|---|-----------|
| 4 | Strong-disorder approximations for ϵ_β. | 13 |
| 5 | Statistics of Green's functions $G_{1,r}$ at large r | 16 |
| 6 | Conclusion | 18 |
| | References | 19 |

1 Introduction

The forward-scattering approximation (FSA) for disordered quantum systems is the simplest approximation for describing the Anderson and many-body localization at strong disorder [1–5]. It takes into account only the *non-repeating paths* connecting two points i and j in the Green's function $G_{ij}(E) = (E - \widehat{H})_{ij}^{-1}$, and only those with the shortest length ('spaths') equal to the distance $r = |i - j|$:

$$G_{ij}(E) = \sum_{\text{spaths}} \prod_{p \in \text{spath}} \frac{V}{E - \epsilon_p}, \quad (1)$$

where $\epsilon_p \in [-W/2, W/2]$ is the box-distributed random on-site energy, and $V = 1$ is the nearest-neighbor hopping amplitude.

The simplest situation is when there is only one path between the points i and j , as it happens in one-dimensional systems and on the Cayley tree. In this case $\ln |G_{ij}(E)| \equiv \ln |G|$ is a sum of $r = |i - j|$ i.i.d. random variables $\ln |V/(E - \epsilon_p)|$, and for the box-shaped distribution of ϵ_p and at $E = 0$ the PDF $P(y = \ln |G|)$ is the Poisson distribution [4]:

$$P_{\text{FSA}}(y = \ln |G|) = \frac{z^{r-1}}{(r-1)!} e^{-z}, \quad z = \ln |G| + r \ln(W/2). \quad (2)$$

The condition of non-repeating paths that does not pass through the same point twice, even along the same set of links, usually applies to strong disorder $W \gg V$. The naive reason for this condition is that increasing the length of the path by an extra link brings about a small factor $V/W \ll 1$. Such a justification, however, ignores completely the possibility of resonances when $|E - \epsilon_i| < V \ll W$. This makes the status of FSA uncertain even at large W/V , especially in the 'loopy' lattices or graphs like a hypercube lattice of Quantum Ising model [6–9] and Quantum Random Energy model [10–12] or its cross-section of XXZ Heisenberg chain [13–19]. In such lattices there are many paths of the same length r which interfere with each other.

The necessity to evaluate the random Green's functions $G_{ij}(E)$ and their distribution function emerges in many problems, of which probably the first was the problem of mesoscopic fluctuations and magneto-resistance in strongly disordered semiconductors [20]. The present interest to FSA is boosted by the study of many-body localized states of disordered interacting systems [2–5].

In this paper we show that even for the Anderson model on a Cayley tree where there is only one geometric path from the initial to the final point, the status of FSA is subtle. The

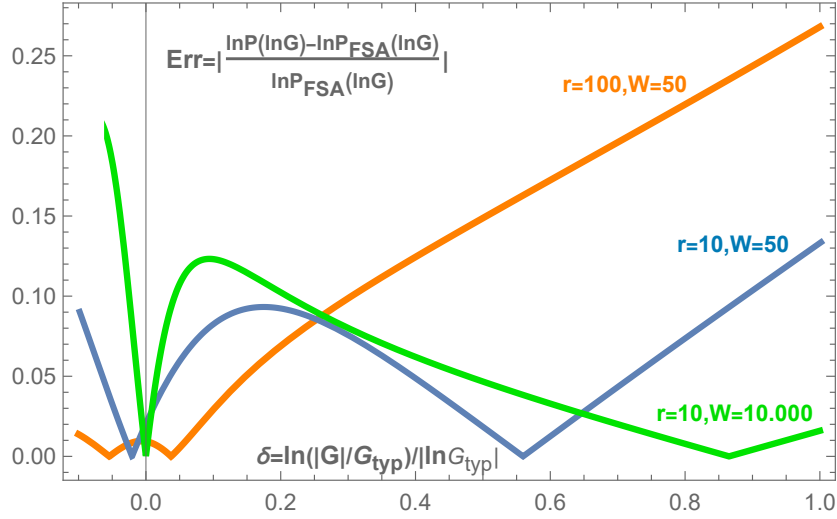


Figure 1: (Color online) **Quality of FSA** The relative error in $\ln P(y = \ln |G|)$ as a function of the relative deviation δ from the typical value G_{typ} for $r = 10$ and $r = 100$ at modestly strong disorder $W = 50$ and for $r = 10$ at extremely strong disorder $W = 10.000$. In all the cases the typical value G_{typ} and the distribution function of $\ln |G|$ at small deviations from it is well described by FSA, while at a sufficiently large deviation ($\delta > 0.05$ at $W = 50$, $r = 100$; $\delta > 0.55$ at $W = 50$ and $r = 10$; $\delta > 0.85$ at $W = 10.000$, $r = 10$) the error changes the sign (resulting in a cusp on a plot of its absolute value) and increases indefinitely as the deviation further grows. Extremely large disorder may delay the onset and reduce the slope of this growth but it does not suppress the error completely. At a large distance $r = |i - j|$ between the points i and j in $G_{ij}(E)$ the overestimation of $\ln P(y = \ln |G|)$ by FSA at large $|G| > G_{typ}$ is greatly enhanced.

typical value $G_{typ} = \exp[\langle \ln |G| \rangle]$ and the distribution function $P(\ln |G|)$ at small deviations from the typical value is described quite well by FSA in all the cases. However, FSA greatly overestimates the probability for sufficiently large deviation from the typical value at $|G| > G_{typ}$ (see Fig. 1), especially at a large distance r between the initial and a final points in the Green's function. By increasing disorder one can suppress this error but for large r it happens only at an unrealistically strong disorder.

The paper consists of three parts. In the first part we show, using the Efetov's supersymmetry method [21], that the moments $m = 2\beta < 1$ of the *real* Green's function $G_{ij}(E)$ on a Cayley tree are *exactly* expressed in terms of the largest eigenvalue ϵ_β of the *linearized* transfer-matrix (TM) equation [22] in the large r limit:

$$\langle |G_{ij}|^{2\beta} \rangle = c_\beta [\epsilon_\beta]^r, \quad (r = |i - j|). \quad (3)$$

This allows to compute the distribution function $P(y = \ln |G|)$ by the Mellin transform in the saddle-point approximation. In the second part, we derive approximate formulas for ϵ_β at large $W \gg 1$. Finally, we compute the distribution function $P(y = \ln |G|)$ at large $W \gg 1$ for different relations between r and W and discuss the accuracy of FSA.

Note that Eq. (3) is important in its own right. The point is that at small and intermediate disorder one has first to solve a non-linear integral equation in order to find a 'renormalized' distribution of on-site energies and only afterwards to solve a linear spectral problem to obtain

ϵ_β for the renormalized distribution of disorder. This renormalization is highly non-trivial, and it is absent in the nonlinear sigma-model (NLSM) version of the problem [23]. The linear spectral problem emerges in the asymptotic regime of TM equation in which certain (Liouvillian) factor in the kernel is dropped. Likewise, Eq. (3) is also valid in the asymptotic regime $r \gg 1$, which, however, looks totally different from that in the TM equation. Yet, it is proven in this paper that it is the same function ϵ_β that controls both the dynamics of the kink solution of TM equation and the moments of Green's functions on a Cayley tree *at any disorder*.

If this non-trivial point is taken for granted, one may guess [24, 25] Eq. (3) from the results of Ref. [26] and Ref. [23]. The first of these works employed the one-step replica symmetry breaking (RSB), while the second one used the super-symmetric NLSM machinery. Despite difference in the methods and interpretation of the results, the basic equations in these two works appeared to be exactly the same. From the identity of these equations one may immediately deduce the close relationship, Eq. (3), between the moments of real Green's functions (entering the formalism of RSB) and the largest eigenvalue ϵ_β of the linearized TM equation (governing the dynamics of the kink solution in the framework of NLSM). In this work we present a formal derivation of Eq. (3) by the supersymmetry method but without the constraint of the NLSM which significantly simplifies the TM equation. Thus our paper proves the validity of Eq. (3) for a Cayley tree with one orbital per site rather than for an infinite number of orbitals per site as in NLSM. An alternative way of justifying Eq. (3) is presented in Ref. [27].

2 TM equation and renormalization of disorder distribution

The model Hamiltonian is given by

$$H = T + V, \quad V_{km} = \varepsilon_k \delta_{km}, \quad T_{mk} = T_{km} \quad (4)$$

where $k, m = 1, \dots, N$, N is the number of graph nodes, and T is the symmetric dimensionless adjacency matrix describing a tree with $K + 1$ nearest neighbors in the bulk (and the root has only K nearest neighbors). We also assume $T_{kk} = 0$. The on-site energies ε_k are distributed according to the distribution function $F(\varepsilon)$.

The retarded(advanced) Green's functions $G_{nm}^\pm(E) \equiv (E - H \pm i\eta)_{nm}^{-1}$ can be represented via functional integral over commuting ($S^{R/A}$) and anti-commuting ($\chi^{R/A}$) variables as follows [21]:

$$G_{nl}^\pm(E) = - \int \prod_k [d\Phi_k d\Phi_k^\dagger] \chi_{R/A}(n) \chi_{R/A}^*(l) e^{-S_0[\Phi, \Phi^\dagger]}, \quad (5)$$

$$S_0[\Phi, \Phi^\dagger] = -i \sum_{mk} \Phi_m^\dagger L (E\delta_{mk} - H_{mk} + i\eta\Lambda\delta_{mk}) \Phi_k$$

where the super-vector Φ_k is defined as:

$$\Phi_k = (S_R(k), \chi_R(k), S_A(k), \chi_A(k))^T, \quad k = 1, \dots, N \quad (6)$$

and the symmetry-breaking matrices $L = \text{diag}\{1, 1, -1, 1\}$ and $\Lambda = \text{diag}\{1, 1, -1, -1\}$. The matrices Λ and L are introduced to ensure correct analytic properties of the Green's

functions (and convergence of the integrals). The measure is defined as

$$[d\Phi_k d\Phi_k^\dagger] \equiv -\frac{d^2 S_R(k) d^2 S_A(k)}{\pi^2} d\chi_R^*(k) d\chi_R(k) d\chi_A^*(k) d\chi_A(k) \quad (7)$$

Using this functional representation one can average over random H_{nm} at an initial stage thus replacing the quadratic in Φ_k action S_0 by the non-quadratic one $S(\Phi, \Phi^\dagger)$ and then to evaluate the generating functional:

$$Y(\Phi_n, \Phi_n^\dagger) = \int \prod_{k \neq n} [d\Phi_k d\Phi_k^\dagger] e^{-S[\Phi, \Phi^\dagger]}, \quad (8)$$

which allows to compute various observables. Remarkably, for one-dimensional systems ($K = 1$) and the Cayley tree ($K > 1$) with one orbital per site this calculation can be done by iterations starting from the boundary of a tree where $Y(\Phi_n, \Phi_n^\dagger) = 1$ and moving towards the root ¹ according to the transfer-matrix equation [22, 28]:

$$\Omega_{r+1}(t, v) = \int_{-\infty}^{\infty} dt' dv' L(t - t', v, v') e^{-e^{t'}} [\Omega_r(t', v')]^K. \quad (9)$$

In Eq. (9) we denote $Y(\Phi_r, \Phi_r^\dagger) \equiv [\Omega_r(t, v)]^{K+1}$ with $e^t = \eta(|S_R|^2 + |S_A|^2)$ and $v = (|S_R|^2 - |S_A|^2)$, and

$$L(t, v, v') = \frac{1}{2\pi} e^{t/2} \cos(v' e^{t/2} + v e^{-t/2}) e^{iE v'} \tilde{F}(v'), \quad (10)$$

where $\tilde{F}(v)$ is the Fourier-transform of the *bare* distribution of on-site energies.

A similar equation can be derived [21, 23, 29] for a NLSM on a Cayley tree which corresponds to an infinite number of orbitals per site. However, in this case, the variables v, v' do not appear in all the equations due to the NLSM constraint $Q^2 = 1$. This is a significant simplification, as in the asymptotic regime $t \rightarrow -\infty$, the self-consistent solution to TM equation can be searched in the simple form $W_{\text{sc}}(t) = 1 + f_\beta e^{\beta t}$, while in the case of one orbital per site considered here it is v -dependent:

$$\Omega_{\text{sc}}(t \rightarrow -\infty, v) = \Omega_0(v) + f_\beta(v) e^{\beta t}, \quad (11)$$

where $\Omega_0(v)$ should be found from the solution of a *non-linear* equation:

$$\Omega_0(v) = \int_{-\infty}^{\infty} dv' \Xi_0(v, v') e^{iE v'} \tilde{F}(v') [\Omega_0(v')]^K, \quad (12)$$

where

$$\Xi_\beta(v, v') = \frac{1}{\pi} \int_0^{+\infty} \frac{dz}{z^{2\beta}} \cos(v' z + v z^{-1}). \quad (13)$$

Then linearizing TM Eq. (9) and omitting the Liouvillian factor e^{-e^t} in the $t \rightarrow -\infty$ asymptotic regime one obtains the spectral problem:

$$\epsilon_\beta f_\beta(v) = \int_{-\infty}^{+\infty} dv' \Xi_\beta(v, v') \tilde{F}(v') e^{iE v'} [\Omega_0(v')]^{K-1} f_\beta(v'). \quad (14)$$

¹The superscript r in this equation enumerates *iterations*; the number that enumerates *generations* on a tree is $R - r$, where R is the total number of generations. The root corresponds to the first generation which is reached after $R - 1$ iterations. In enumerating the *nodes* of a tree it is natural to denote the root by $n = 1$.

The solution to this spectral problem determines the velocity $v_\beta = \beta^{-1} \ln(K\epsilon_\beta)$ of the kink solution to the TM equation in the delocalized phase which minimization with respect to β yields the fractal dimension of the wave function $D = 2 - D_0 = \min_\beta[v_\beta]/\ln K$ determining its support set volume $\sim N^D$ [23, 26].

The form of Eq. (14) immediately suggests the physical meaning of the factor $[\Omega_0(v)]^{K-1}$ as the factor that renormalizes the Fourier-transform of the on-side disorder distribution:

$$\tilde{\mathcal{F}}(v) = \tilde{F}(v) [\Omega_0(v)]^{K-1}. \quad (15)$$

Eq. (15) shows that such a renormalization is absent in two special cases: (i) one-dimensional system $K = 1$, and (ii) the NLSM on the Cayley tree $\Omega_0(v) = 1$. In the second case the eigenvalue ϵ_β does not depend on the branching number K of the tree.

It is instructive to show application of Eqs. (12), (15) to the exactly solvable case of the Cauchy distribution $\tilde{F}(v) = e^{-(W/2)|v|}$. At $\beta = 0$ Eq. (13) results in a singular kernel:

$$\Xi_0(v, v') = \delta(v') - \theta(vv') \sqrt{\left|\frac{v}{v'}\right|} J_1(2\sqrt{|vv'|}). \quad (16)$$

One can easily find a solution to Eq. (12) in a form $\Omega_0 = e^{-\kappa|v|}$, with

$$\kappa = \frac{\sqrt{(W/2)^2 + 4K} - (W/2)}{2K} \quad (17)$$

Then Eq. (15) gives rise to $\tilde{\mathcal{F}}(v) = e^{-(W_R/2)|v|}$ of the same Cauchy form with the renormalized "disorder strength":

$$W_R = \frac{1}{2K} \left((K+1)W + (K-1)\sqrt{W^2 + 16K} \right), \quad (18)$$

which at $K > 1$ remains finite as the "physical disorder" W tends to zero.

The physical meaning of the renormalization, Eqs. (15), (18), is related to the remnant of ballistic motion in the disordered system. It is especially important at small disorder $W \lesssim 1$. In particular this renormalization is responsible for a finite derivative $\partial_\beta \epsilon_\beta|_{\beta=0} = -\ln K$ which results in a finite Lyapunov exponent $\lambda_{typ} = -(1/2)\partial_\beta \epsilon_\beta|_{\beta=0}$ [26] at a vanishing disorder $W \rightarrow 0$ in the case of a Cayley tree with one orbital per node. In the case of NLSM on a Cayley tree, where the renormalization is absent, the Lyapunov exponent tends to zero in the limit $W \rightarrow 0$, as well as in a one-dimensional system. This peculiarity of NLSM on a Cayley tree leads to an existence of an ergodic state at a finite disorder strength [23], while the states are non-ergodic down to $W = 0$ on a disordered Cayley tree with one orbital per site [26, 27].

3 Moments of real Green's functions

The focus of our interest in this paper is the moment I_β the absolute value of a real Green's function $G_{nm}(E)$:

$$I_\beta = \left\langle |G_{nm}(E)|^{2\beta} \right\rangle, \quad 0 < \beta < 1/2. \quad (19)$$

In the absence of degeneracy of spectrum, Green's functions have simple poles at any $E = E_n$, where E_n is an eigenenergy in a finite system. Upon averaging over disorder at a fixed E

the levels pass through the energy E just causing very large values of $|G_{nm}(E)|$. This gives rise to a power-law tail of the distribution function $P(x = |G|) \sim \langle \delta(x - |G_{nm}(E)|) \rangle \approx \int dE_k \delta(x - |E - E_k|^{-1}) \sim 1/G^2$. Such a tail makes the moments of Green's functions of order $2\beta \geq 1$ divergent. At the same time the moments of real Green's functions of order $2\beta < 1$ are well-defined and at a finite system size N are given by the limit $\eta \rightarrow 0$ of the corresponding moment of G^+G^- involving complex Green's functions $G_{nm}^\pm(E)$:

$$I_\beta = \lim_{\eta \rightarrow 0} \left\langle |G_{nm}^+(E)G_{nm}^-(E)|^\beta \right\rangle, \quad 0 < \beta < 1/2. \quad (20)$$

Now, using the functional representation Eq. (5) of retarded and advanced Green's functions, introducing average the product $[G_{nm}^+(E)]^\beta [G_{nn}^-(E)]^\beta$ over the diagonal disorder and $a = 1, 2, \dots, \beta$ copies of the system we express:

$$\langle [G_{nl}^+(E)]^\beta [G_{nl}^-(E)]^\beta \rangle = \int \left(\prod_{ka} [d\Phi_k^{(a)} d\Phi_k^{(a)\dagger}] \right) \prod_a \chi_R^{(a)*}(l) \chi_R^{(a)}(n) \chi_A^{(a)}(n) \chi_A^{(a)*}(l) e^{-S[\Phi, \Phi^\dagger]}, \quad (21)$$

$$S[\Phi, \Phi^\dagger] = - \sum_m \ln \tilde{F} \left(\sum_a \Phi_m^{(a)\dagger} L \Phi_m^{(a)} \right) - i \sum_{mka} \Phi_m^{(a)\dagger} L (E \delta_{mk} - T_{mk} + i\eta \Lambda \delta_{mk}) \Phi_k^{(a)} \quad (22)$$

3.1 Integration over the phases

Let us first integrate over phases $\phi_{R/A}^{(a)}(k)$ of complex variables $S_{R/A}^{(a)}(k)$. To accomplish that, one can first notice that T is real and symmetric. Thus, one can rearrange the hopping term in the action as

$$\begin{aligned} \sum_{mka} T_{mk} \Phi_m^{(a)\dagger} L \Phi_k^{(a)} &= \sum_{mka} T_{mk} \operatorname{Re} \{ S_R^{(a)*}(m) S_R^{(a)}(k) - \\ & S_A^{(a)*}(m) S_A^{(a)}(k) \} + \sum_{mka} T_{mk} \left(\chi_R^{(a)*}(m) \chi_R^{(a)}(k) + \chi_A^{(a)*}(m) \chi_A^{(a)}(k) \right) \end{aligned} \quad (23)$$

which suggests to switch to the modulus and the phase of the complex variables $S_{R/A}^{(a)}(k) = |S_{R/A}^{(a)}(k)| e^{i\phi_{R/A}^{(a)}(k)}$. The non-Grassmann part of the hopping term can be written as

$$\begin{aligned} & \sum_{mka} T_{mk} \operatorname{Re} \{ S_R^{(a)*}(m) S_R^{(a)}(k) - S_A^{(a)*}(m) S_A^{(a)}(k) \} \\ &= \sum_{mka} T_{mk} \left\{ |S_R^{(a)}(m)| |S_R^{(a)}(k)| \cos(\phi_R^{(a)}(m) - \phi_R^{(a)}(k)) - (R \rightarrow A) \right\} \end{aligned} \quad (24)$$

Then evaluating integrals over phases and introducing new variables:

$$\left| S_R^{(a)}(k) \right|^2 \equiv s_k^{(a)}, \quad \left| S_A^{(a)}(k) \right|^2 \equiv \tilde{s}_k^{(a)} \quad (25)$$

we obtain:

$$\begin{aligned}
\langle [G_{nl}^+(E)]^\beta [G_{nl}^-(E)]^\beta \rangle &= \int \left(\prod_{ka} ds_k^{(a)} d\tilde{s}_k^{(a)} d\chi_R^{(a)}(k) d\chi_R^{(a)*}(k) d\chi_A^{(a)*}(k) d\chi_A^{(a)}(k) \right) e^{-S_1[s, \chi]} \times \\
&\quad \times \prod_a \chi_R^{(a)*}(l) \chi_R^{(a)}(n) \chi_A^{(a)}(n) \chi_A^{(a)*}(l) \times \\
&\quad \times \prod_{\langle km \rangle} J_0 \left(2\sqrt{s_k^{(a)} s_m^{(a)}} \right) J_0 \left(2\sqrt{\tilde{s}_k^{(a)} \tilde{s}_m^{(a)}} \right) e^{-i(\chi_R^{(a)*}(m) \chi_R^{(a)}(k) + \chi_A^{(a)*}(m) \chi_A^{(a)}(k) + sym.)} \quad (26)
\end{aligned}$$

where the diagonal part of the action reads as

$$\begin{aligned}
S_1[s, \chi] &= - \sum_m \ln \tilde{F} \left(\sum_a \left[s_m^{(a)} - \tilde{s}_m^{(a)} + \chi_R^{(a)*}(m) \chi_R^{(a)}(m) + \chi_A^{(a)*}(m) \chi_A^{(a)}(m) \right] \right) - \\
&\quad - iE \sum_{ma} \left(s_m^{(a)} - \tilde{s}_m^{(a)} + \chi_R^{(a)*}(m) \chi_R^{(a)}(m) + \chi_A^{(a)*}(m) \chi_A^{(a)}(m) \right) + \eta \sum_{ma} \left(s_m^{(a)} + \tilde{s}_m^{(a)} \right) \quad (27)
\end{aligned}$$

We have dropped the Grassmann term with η in front of it.

3.2 Integration over anti-commuting variables

Next, we perform a shift of variables

$$\begin{aligned}
s_m^{(a)} &\rightarrow s_m^{(a)} - \chi_R^{(a)*}(m) \chi_R^{(a)}(m), \\
\tilde{s}_m^{(a)} &\rightarrow \tilde{s}_m^{(a)} + \chi_A^{(a)*}(m) \chi_A^{(a)}(m) \quad (28)
\end{aligned}$$

The domain of integration is correctly captured if one writes down the transformed step functions in the integration measure explicitly as

$$\begin{aligned}
\theta(s_m^{(a)}) &\rightarrow \theta(s_m^{(a)}) - \delta(s_m^{(a)}) \chi_R^{(a)*}(m) \chi_R^{(a)}(m), \\
\theta(\tilde{s}_m^{(a)}) &\rightarrow \theta(\tilde{s}_m^{(a)}) + \delta(\tilde{s}_m^{(a)}) \chi_A^{(a)*}(m) \chi_A^{(a)}(m) \quad (29)
\end{aligned}$$

The advantage of this shift is that it removes the anti-commuting variables from the diagonal part of the action in (27). The integration over anti-commuting variables in Eqs. (26), (27) factorizes as $M = \prod_a M_a^R M_a^A$, where

$$\begin{aligned}
M_a^R &= \int \prod_k \left(d\chi_R^{(a)}(k) d\chi_R^{(a)*}(k) \right) \chi_R^{(a)*}(l) \chi_R^{(a)}(n) \prod_m \left(\theta(s_m^{(a)}) - \delta(s_m^{(a)}) \chi_R^{(a)*}(m) \chi_R^{(a)}(m) \right) \times \\
&\quad \times \prod_{\langle km \rangle} J_0 \left(2\sqrt{(s_k^{(a)} - \chi_R^{(a)*}(k) \chi_R^{(a)}(k)) (s_m^{(a)} - \chi_R^{(a)*}(m) \chi_R^{(a)}(m))} \right) e^{-i(\chi_R^{(a)*}(m) \chi_R^{(a)}(k) + sym.)} \quad (30)
\end{aligned}$$

and

$$\begin{aligned}
M_a^A &= \int \prod_k \left(d\chi_A^{(a)*}(k) d\chi_A^{(a)}(k) \right) \chi_A^{(a)}(n) \chi_A^{(a)*}(l) \prod_m \left(\theta(\tilde{s}_m^{(a)}) + \delta(\tilde{s}_m^{(a)}) \chi_A^{(a)*}(m) \chi_A^{(a)}(m) \right) \times \\
&\quad \times \prod_{\langle km \rangle} J_0 \left(2\sqrt{(\tilde{s}_k^{(a)} + \chi_A^{(a)*}(k) \chi_A^{(a)}(k)) (\tilde{s}_m^{(a)} + \chi_A^{(a)*}(m) \chi_A^{(a)}(m))} \right) e^{-i(\chi_A^{(a)*}(m) \chi_A^{(a)}(k) + sym.)} \quad (31)
\end{aligned}$$

Let us assume that the initial point $n = 1$ is a root of a tree. All the anti-commuting variables in the integral Eq. (30) are divided in two parts: those which correspond to sites on the (unique) path \mathcal{P}_l from the root to the final point l and the remaining variables. Let us first consider integration over the anti-commuting variables of the first part. The result is given only by the saturated (i.e. that have exactly one pair of variables $\chi\chi^*$ corresponding to any copy (a) and any site p) set of variables in the expansion of exponent in Eq. (30) and the 'source' variables $\chi_{R/A}^{(a)*}(l)\chi_{R/A}^{(a)}(n)$. The integration over retarded variables gives $i^{|\mathcal{P}_l|}$, and the advanced components produce the factor $(-i)^{|\mathcal{P}_l|}$ (where $|\mathcal{P}_l|$ is the length of the path), so they compensate each other (note the order of anti-commuting variables in the measure and in the pre-factor!).

Notice that, since the integrals along the path \mathcal{P}_l are already saturated, the hopping terms in the exponent of Eqs. (30), (31) connecting the remaining branches of the tree and the path \mathcal{P}_l can be omitted. Therefore, our final step is to integrate over all possible anti-commuting variables of 'decoupled' branches. This task can be accomplished iteratively.

Let us start from the boundary. We are going to use the following short notation: χ^* and χ will denote the anti-commuting variables that we are currently integrating over, while ζ^* and ζ will stand for the variables belonging to the unique predecessor of the chosen site. Therefore, we need to compute the following integral:

$$\begin{aligned} \tilde{\Xi}_0(s, s') = & \int d\chi d\chi^* [\theta(s') + \delta(s')\chi^*\chi] \times \\ & \times J_0 \left(2\sqrt{ss'} + \left(\sqrt{\frac{s'}{s}}\zeta^*\zeta + \sqrt{\frac{s}{s'}}\chi^*\chi \right) + \frac{1}{2\sqrt{ss'}}\chi^*\chi\zeta^*\zeta \right) e^{-i\zeta^*\chi - i\chi^*\zeta} \end{aligned} \quad (32)$$

where $e^{-i\zeta^*\chi - i\chi^*\zeta} = 1 - i(\zeta^*\chi + \chi^*\zeta) + \chi^*\chi\zeta^*\zeta$. The integral Eq. (32) is equal, up to an overall opposite sign, to a single integral in M_a^A . A remarkable fact is that this integral, in fact, does not depend on ζ and ζ^* .

Indeed, expanding the Bessel functions in the anti-commuting variables, combining the result with the expansion of the exponential term and using the identity for Bessel functions $J_2(x) - J_0(x) - 2\frac{J_1(x)}{x} = -2J_0(x)$ one can easily see that the contribution proportional to $\zeta^*\zeta$ is canceled out, and the remaining integral leads to

$$\tilde{\Xi}_0(s, s') = \delta(s') - \theta(s')\sqrt{\frac{s}{s'}} J_1(2\sqrt{ss'}) \quad (33)$$

The integral over retarded variables can be performed in a similar way. As a result, the total contribution from the anti-commuting variables has the following form:

$$M = \prod_a \prod_{\substack{\langle mk \rangle \\ m, k \in \mathcal{P}_l}} \left(J_0 \left(2\sqrt{s_m^{(a)} s_k^{(a)}} \right) J_0 \left(2\sqrt{\tilde{s}_m^{(a)} \tilde{s}_k^{(a)}} \right) \right) \prod_{\substack{\langle mk \rangle \\ m, k \notin \mathcal{P}_l}} \left(\tilde{\Xi}_0(s_m^{(a)}, s_k^{(a)}) \tilde{\Xi}_0(\tilde{s}_m^{(a)}, \tilde{s}_k^{(a)}) \right) \quad (34)$$

Note that $\tilde{\Xi}_0(s_k, s_m)$ is not symmetric, so we always assume that the site k (corresponding to the first argument s_k) is closer to the root than the site m corresponding to the second argument s_m .

Finally, one can represent the average of interest solely in terms of the conventional integrals over $s_k^{(a)}$ and $\tilde{s}_k^{(a)}$ as:

$$\begin{aligned} \langle [G_{nl}^+(E)]^\beta [G_{nl}^-(E)]^\beta \rangle &= \int \left(\prod_{ka} ds_k^{(a)} d\tilde{s}_k^{(a)} \theta(s_k^{(a)}) \theta(\tilde{s}_k^{(a)}) \right) e^{-S_1[s,0]} \times \\ &\times \prod_a \prod_{\langle mk \rangle} \left(J_0 \left(2\sqrt{s_m^{(a)} s_k^{(a)}} \right) J_0 \left(2\sqrt{\tilde{s}_m^{(a)} \tilde{s}_k^{(a)}} \right) \right) \prod_{\langle mk \rangle} \left(\tilde{\Xi}_0(s_m^{(a)}, s_k^{(a)}) \tilde{\Xi}_0(\tilde{s}_m^{(a)}, \tilde{s}_k^{(a)}) \right) \end{aligned} \quad (35)$$

At this moment, we are left with 2β real variables at each node. The goal of the next section is to reduce this set to a single variable, β appearing as a parameter in the integrand. If this goal is accomplished, one can easily make an analytic continuation over β .

3.3 Integration over s_k and \tilde{s}_k

Our next step is to integrate over s_k and \tilde{s}_k . This can be done by means of the following identity

$$1 = \prod_m \int_{-\infty}^{+\infty} dv_m \delta \left(v_m - \sum_a \left[s_m^{(a)} - \tilde{s}_m^{(a)} \right] \right) = \prod_m \int_{-\infty}^{+\infty} \frac{dv_m dz_m}{2\pi} e^{iz_m \left(v_m - \sum_a \left[s_m^{(a)} - \tilde{s}_m^{(a)} \right] \right)} \quad (36)$$

In terms of these new variables, the action reads as

$$S_1[s, 0] = - \sum_m \ln \tilde{F}(v_m) - iE \sum_m v_m + \eta \sum_{ma} \left(s_m^{(a)} + \tilde{s}_m^{(a)} \right) \quad (37)$$

Now we are in a position to integrate over s_k and \tilde{s}_k because they are decoupled from each other. The integration can again be performed iteratively, starting from the boundary (once again, we assume that $n \equiv 1$ is the root of the tree).

First of all, one can easily verify that:

$$\int_0^{+\infty} ds_k^{(a)} e^{-i(z_k - i\eta)s_k^{(a)}} \tilde{\Xi}_0 \left(s_m^{(a)}, s_k^{(a)} \right) = e^{\frac{is_m^{(a)}}{z_k - i\eta}} \quad (38)$$

Thus, the complete integration over 2β initial real variables for a given node at the boundary is given by

$$e^{\frac{iz_k}{z_k^2 + \eta^2} \sum_a \left[s_m^{(a)} - \tilde{s}_m^{(a)} \right] - \frac{\eta}{z_k^2 + \eta^2} \sum_a \left[s_m^{(a)} + \tilde{s}_m^{(a)} \right]} \quad (39)$$

where $\sum_a \left[s_m^{(a)} - \tilde{s}_m^{(a)} \right]$ can be replaced by v_m due to the presence of the delta function (36).

Moreover, as it will be explained later, one can safely set $\eta = 0$.

Next, by combining this new term with $e^{iz_k v_k}$ and integrating over z_k , we obtain the effective kernel operating on a given link which does not belong to the path \mathcal{P}_l :

$$\begin{aligned}\Xi_0(v_m, v_k) &= \frac{1}{2\pi} \int_{-\infty}^{+\infty} dz e^{i(vz^{-1} + v'z)} = \frac{1}{\pi} \int_0^{+\infty} dz \cos(vz^{-1} + v'z) = \\ &= \delta(v_k) - \theta(v_k v_m) \sqrt{\frac{|v_m|}{|v_k|}} J_1\left(2\sqrt{|v_m||v_k|}\right)\end{aligned}\quad (40)$$

Remarkably, it coincides with the kernel of the non-linear equation (16). This process can be continued further, involving other links that do not belong to the path \mathcal{P}_l . The integration along the path \mathcal{P}_l is only slightly different. We make use of the following integral

$$\int_0^{+\infty} ds_k^{(a)} e^{-i(z_k - i\eta)s_k^{(a)}} J_0\left(2\sqrt{s_m^{(a)} s_k^{(a)}}\right) = \frac{-i}{z_k - i\eta} e^{\frac{is_m^{(a)}}{z_k - i\eta}} \quad (41)$$

Therefore, the integration over $s_k^{(a)}$ leads to

$$\frac{1}{(z_k^2 + \eta^2)^\beta} e^{\frac{iz_k}{z_k^2 + \eta^2} \sum_a [s_m^{(a)} - \tilde{s}_m^{(a)}] - \frac{\eta}{z_k^2 + \eta^2} \sum_a [s_m^{(a)} + \tilde{s}_m^{(a)}]} \quad (42)$$

where $\sum_a [s_m^{(a)} - \tilde{s}_m^{(a)}]$ can again be replaced by v_m due to the presence of the delta function (36). We also denote here $l_m = \sum_a [s_m^{(a)} + \tilde{s}_m^{(a)}]$.

By combining the resulting expression with $e^{iz_k v_k}$, we obtain the following integral over z_k

$$\mathcal{R}(v_m, l_m | v_k) = \int_{-\infty}^{+\infty} \frac{dz_k}{(z_k^2 + \eta^2)^\beta} e^{\frac{iz_k v_m}{z_k^2 + \eta^2} - \frac{\eta l_m}{z_k^2 + \eta^2} + iz_k v_k} \quad (43)$$

Crucially, this expression is an analytic function of β , and thus, we are in a position to analytically continue it to the region $\beta < 1/2$. This procedure makes the integral over z_k convergent even at $\eta = 0$ and justifies the limit $\eta = 0$ in Eqs. (39), (42) which eliminates the dependence on l_m whatsoever. Indeed, in the course of the subsequent integration over s_m and \tilde{s}_m the dominant region $s_m, \tilde{s}_m \sim z_m^{-1}$ is finite in the limit $\eta \rightarrow 0$ due to the convergence of the integral over z_m .

One obtains the effective β -dependent kernel operating on a given link belonging to the path \mathcal{P}_l :

$$\Xi_\beta(v, v') = \frac{1}{\pi} \int_0^{+\infty} \frac{dz}{|z|^{2\beta}} \cos(vz^{-1} + v'z) \quad (44)$$

which coincides with the kernel (13) in the linear eigenvalue problem Eq. (14).

This integral can be evaluated exactly as follows

$$\begin{aligned}\Xi_\beta(v, v') &= \frac{2}{\pi} \left(\frac{|v|}{|v'|}\right)^{\frac{1}{2}-\beta} \left\{ \theta(-vv') \sin(\pi\beta) K_{1-2\beta}\left(2\sqrt{|v'v|}\right) + \right. \\ &\quad \left. + \frac{\pi\theta(vv')}{4\cos(\pi\beta)} \left(J_{2\beta-1}\left(2\sqrt{|v'v|}\right) - J_{1-2\beta}\left(2\sqrt{|v'v|}\right) \right) \right\}\end{aligned}\quad (45)$$

The last remaining integration over the root $n = 1$ can be performed in the same way as in Eq. (41) by setting all $s_m^{(a)}$ to zero (since the root has no predecessor). Thus, the integral over z_1 leads to

$$\frac{1}{2\pi} \int_{-\infty}^{+\infty} \frac{dz_1}{(z_1^2 + \eta^2)^\beta} e^{iz_1 v_1} = \frac{|v_1|^{2\beta-1}}{2 \cos(\pi\beta)\Gamma(2\beta)}, \quad \eta \rightarrow 0^+ \quad (46)$$

The final expression reads as follows:

$$\begin{aligned} \langle [G_{nl}^+(E)]^\beta [G_{nl}^-(E)]^\beta \rangle &= \frac{1}{2 \cos(\pi\beta)\Gamma(2\beta)} \int_{-\infty}^{+\infty} \left(\prod_k dv_k \tilde{F}(v_k) e^{iEv_k} \right) |v_1|^{2\beta-1} \times \\ &\times \prod_{\substack{\langle mk \rangle \\ m, k \in \mathcal{P}_l}} \Xi_\beta(v_m, v_k) \prod_{\substack{\langle mk \rangle \\ m, k \notin \mathcal{P}_l}} \Xi_0(v_m, v_k) \quad (47) \end{aligned}$$

3.4 Iterative representation of the result

The multiple integral Eq. (47) can be represented in a form of iterations, similar to the TM equation. To this end we introduce two functions $\Psi_0^{(r)}(v)$ and $\Psi_\beta^{(r)}(v)$ obeying the following recursive equations:

$$\Psi_0^{(r+1)}(v) = \int_{-\infty}^{+\infty} dv' \Xi_0(v, v') \tilde{F}(v') e^{iEv'} [\Psi_0^{(r)}(v')]^K, \quad (48)$$

with the initial condition $\Psi_0^{(0)}(v) \equiv 1$, and

$$\Psi_\beta^{(r+1)}(v) = \int_{-\infty}^{+\infty} dv' \Xi_\beta(v, v') \tilde{F}(v') e^{iEv'} \Psi_\beta^{(r)}(v') \left[\Psi_0^{(R-|\mathcal{P}_l|-1+s)}(v') \right]^{K-1}, \quad (49)$$

with the initial condition $\Psi_\beta^{(0)}(v) \equiv \Psi_0^{(R-|\mathcal{P}_l|-1)}(v)$. Here R is the total number of generations on the tree and $|\mathcal{P}_l|$ is the length of the path \mathcal{P}_l .

The function $\Psi_0^{(r)}(v)$ describes the summation over the tree branch with r generations which the path \mathcal{P}_l does not belong to. One can immediately recognize in Eq. (48) the non-linear equation, Eq. (12), for the zero-order approximation of the TM equation with the same initial condition. Thus the self-consistent solution to Eq. (48) is $\Psi_0(v) \equiv \Omega_0(v)$. On the other hand, the function $\Psi_\beta^{(r)}(v)$ is related to the summation over the part of the path \mathcal{P}_l of the length r .

Then the result of the previous subsection Eq. (47) can be expressed through these functions as:

$$\langle |G_{1l}(E)|^{2\beta} \rangle = \frac{1}{2 \cos(\pi\beta)\Gamma(2\beta)} \int_{-\infty}^{+\infty} dv |v|^{2\beta-1} \tilde{F}(v) e^{iEv} \Psi_\beta^{(|\mathcal{P}_l|)}(v) \left[\Psi_0^{(R-1)}(v) \right]^{K-1}, \quad (50)$$

Let us now assume the separation of scales with the following order $1 \ll |\mathcal{P}_l| \ll R$. Then, after many consequent integrations, the generating function $\Psi_0^{(R-|\mathcal{P}_l|-1)}(v)$ can be replaced by $\Omega_0(v)$ which is the self-consistent solution of Eq. (12). Moreover, in the integrations along \mathcal{P}_l , only the right eigenfunction with the largest eigenvalue $\epsilon_\beta = \max_\kappa \{\epsilon_\beta^{(\kappa)}\}$ survives, which can be found as usual from the equation:

$$\epsilon_\beta^{(\kappa)} f_\beta^{(\kappa)}(v) = \int_{-\infty}^{+\infty} dv' \Xi_\beta(v, v') \tilde{\mathcal{F}}(v') e^{iEv'} f_\beta^{(\kappa)}(v'), \quad (51)$$

where $\tilde{\mathcal{F}}$ is the renormalized Fourier-transform of the on-site disorder distribution obeying Eq. (15). Therefore

$$\Psi_\beta^{(|\mathcal{P}_l|)}(v) \approx (\epsilon_\beta)^{|\mathcal{P}_l|} C_\beta f_\beta(v) \quad (52)$$

where C_β is the coefficient in the decomposition of the initial condition $\Omega_0(v)$ in terms of the left eigenfunctions

$$C_\beta = \int_{-\infty}^{+\infty} dv g_\beta(v) \Omega_0(v) \quad (53)$$

and $g_\beta(v)$ corresponds to the same largest eigenvalue

$$\epsilon_\beta g_\beta(v) = \tilde{\mathcal{F}}(v) e^{iEv} \int_{-\infty}^{+\infty} dv' g_\beta(v') \Xi_\beta(v', v), \quad (54)$$

and we assumed that there is a finite gap between the largest eigenvalue ϵ_β and the second largest eigenvalue. Finally, we obtain

$$\langle |G_{ll}(E)|^{2\beta} \rangle = (\epsilon_\beta)^{|\mathcal{P}_l|} \varkappa_\beta, \quad |\mathcal{P}_l|, R \rightarrow \infty, \quad |\mathcal{P}_l|/R \rightarrow 0 \quad (55)$$

where

$$\varkappa_\beta = \frac{C_\beta}{2 \cos(\pi\beta) \Gamma(2\beta)} \int_{-\infty}^{+\infty} dv |v|^{2\beta-1} \tilde{\mathcal{F}}(v) e^{iEv} f_\beta(v). \quad (56)$$

Eqs. (55), (56) is the main result of Section III and the main technical result of this paper.

4 Strong-disorder approximations for ϵ_β .

In this section we derive simple approximations for ϵ_β and control their accuracy. The idea is that at strong disorder the renormalization of the on-site energy distribution is weak and at sufficiently large W can be neglected. In order to show this we note that the integral part of Eq. (12) converges at $|v'| \sim W^{-1} \ll 1$ due to the factor $\tilde{F}(v')$. The argument of function $\Omega_0(v)$ entering the spectral problem Eq. (14) is also effectively restricted by a similar factor in this equation. This allows to expand the Bessel function in the kernel of Eq. (12) and represent the kernel as a sum of the factorized ones which makes the equation solvable. Expansion of the Bessel function to the lowest order in its argument then leads to the solution:

$$\Omega_0(v) \approx 1 - |v| \frac{\int dv' \tilde{F}(v')}{1 + K \int dv' |v'| \tilde{F}(v')} = 1 + O(1/W^2). \quad (57)$$

This solution shows that the renormalized distribution $\mathcal{F}(\varepsilon)$, Eq. (15), acquires a $1/\varepsilon^2$ tail for any bare distribution (with the convergent mean value) which decreases at large ε faster than or similar to $1/\varepsilon^2$. In this paper we consider three such distributions, the box-shaped distribution, the Gauss distribution and the Cauchy distribution which Fourier transforms read as follows:

$$F_b(\varepsilon) = \frac{\theta(|\varepsilon| - W/2)}{W}, \quad \tilde{F}_b(v) = \frac{2 \sin(W v/2)}{(W v)}, \quad (58)$$

$$F_G(\varepsilon) = \frac{1}{\sqrt{\pi W^2}} e^{-\varepsilon^2/W^2}, \quad \tilde{F}_G(v) = e^{-(W/4)^2 v^2}, \quad (59)$$

$$F_C(\varepsilon) = \frac{(W/2\pi)}{\varepsilon^2 + (W/2)^2}, \quad \tilde{F}_C(v) = e^{-(W/2)|v|}. \quad (60)$$

As is said before, any of these bare distributions acquire a tail A/ε^2 ; however, the prefactor A is small, e.g. for the box distribution:

$$A_{\text{box}} = \frac{\pi}{W + 4K/W}. \quad (61)$$

The simplest approximation at large disorder is to neglect this renormalization whatsoever: $\Omega_0 = 1$.

With this assumption, expanding the Bessel functions in the kernel of Eq. (51), one obtains a 2×2 matrix eigenvalue problem:

$$\begin{aligned} \epsilon_\beta I_1 &= \frac{\sin(\pi\beta)}{\pi} \Gamma(1 - 2\beta) I_2 \int dv' \tilde{F}(v') + \frac{\sin(\pi\beta)}{\pi} \Gamma(2\beta - 1) I_1 \int dv' \tilde{F}(v') |v'|^{1-2\beta} \\ \epsilon_\beta I_2 &= \frac{\sin(\pi\beta)}{\pi} \Gamma(1 - 2\beta) I_2 \int dv' \tilde{F}(v') |v'|^{2\beta-1} + \frac{\sin(\pi\beta)}{\pi} \Gamma(2\beta - 1) I_1 \int dv' \tilde{F}(v'), \end{aligned}$$

where

$$I_1 = \int dv \tilde{F}(v) f_\beta(v), \quad I_2 = \int dv |v|^{2\beta-1} \tilde{F}(v) f_\beta(v)$$

One can see that in this approximation there are two eigenvalues of which the largest is:

- For the box distribution:

$$\begin{aligned} \epsilon_\beta &= \frac{1}{W |1 - 2\beta|} \left\{ \text{sign}(1 - 2\beta) \left[\left(\frac{W}{2}\right)^{1-2\beta} - \left(\frac{W}{2}\right)^{2\beta-1} \right] + \right. \\ &\quad \left. + \sqrt{\left[\left(\frac{W}{2}\right)^{1-2\beta} + \left(\frac{W}{2}\right)^{2\beta-1} \right]^2 - 2\pi (1 - 2\beta) \tan(\pi\beta)} \right\}. \quad (62) \end{aligned}$$

- For the Gaussian distribution:

$$\begin{aligned} \epsilon_\beta &= -\frac{\sqrt{\pi}}{(\frac{1}{2} - \beta) \cos(\pi\beta) W} \left\{ \frac{(\frac{W}{2})^{1-2\beta}}{\Gamma(\beta - \frac{1}{2})} + \frac{(\frac{W}{2})^{2\beta-1}}{\Gamma(\frac{1}{2} - \beta)} - \right. \\ &\quad \left. - \sqrt{\left[\frac{(\frac{W}{2})^{1-2\beta}}{\Gamma(\beta - \frac{1}{2})} - \frac{(\frac{W}{2})^{2\beta-1}}{\Gamma(\frac{1}{2} - \beta)} \right]^2 - \frac{1 - 2\beta}{\pi} \sin(2\pi\beta)} \right\}. \quad (63) \end{aligned}$$

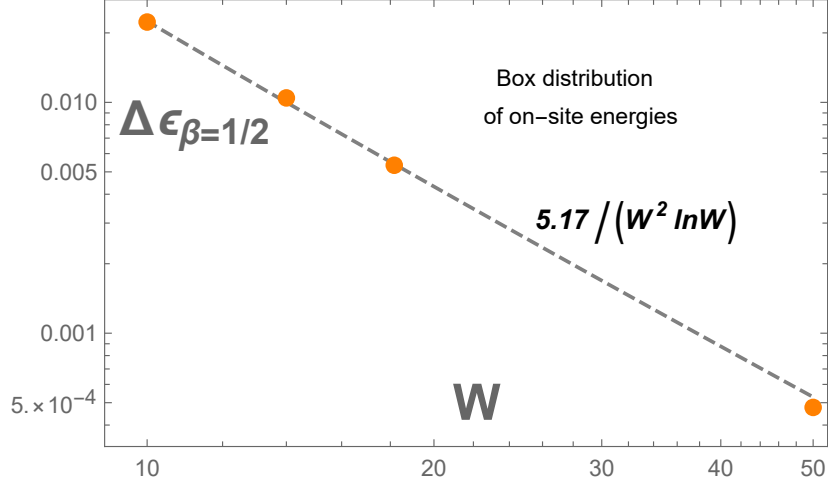


Figure 2: (Color online) **The accuracy of approximation for ϵ_β , Eq. (62), for the box distribution of on-site energies at large disorder $W \gg 1$.** The difference $\Delta\epsilon_\beta$ between the numerical solution for $\epsilon_{\beta=1/2}$ of the exact Eqs. (12), (14) and the approximate solution for $\epsilon_{\beta=1/2}$, Eq. (62), as a function of disorder strength W for a $K = 2$ Cayley tree.

- For the Cauchy distribution:

$$\begin{aligned} \epsilon_\beta &= \frac{1}{W |\cos(\pi\beta)|} \left\{ \text{sign}(1-2\beta) \left[\left(\frac{W}{2}\right)^{1-2\beta} - \left(\frac{W}{2}\right)^{2\beta-1} \right] + \right. \\ &\quad \left. + \sqrt{\left[\left(\frac{W}{2}\right)^{1-2\beta} + \left(\frac{W}{2}\right)^{2\beta-1} \right]^2 - \frac{4 \sin(2\pi\beta)}{\pi(1-2\beta)}} \right\} \end{aligned} \quad (64)$$

One can see that all those expressions for ϵ_β respect the basic (ACTA) symmetry discovered in a seminal work of Abou-Chacra, Thouless and Anderson [22]:

$$\epsilon_\beta = \epsilon_{1-\beta}. \quad (65)$$

Furthermore, Eqs. (62)-(64) respect the exact property of ϵ_β :

$$\epsilon_{\beta=0} = 1. \quad (66)$$

Note that earlier in Refs. [23, 26] there was proposed another approximation for ϵ_β at large disorder for the box distribution:

$$\epsilon_\beta \approx \frac{(W/2)^{1-2\beta} - (W/2)^{2\beta-1}}{(W/2 - 2/W)(1-2\beta)}. \quad (67)$$

The accuracy of this simple approximation is $O(W \ln W)^{-1}$, while the accuracy of Eqs. (62) and (63) is much higher (see Fig. 2 and Fig. 3):

$$\Delta\epsilon_{\beta=1/2} = O(W^2 \ln W)^{-1}. \quad (68)$$

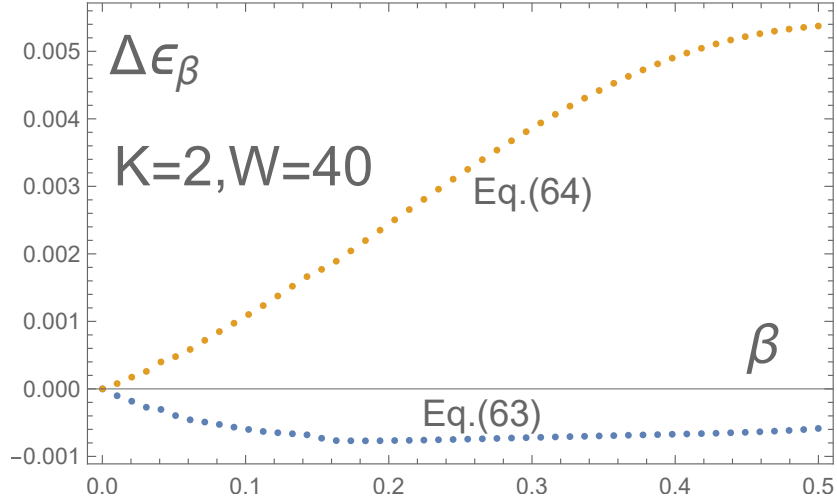


Figure 3: (Color online) **Comparison of the accuracy of approximation for ϵ_β by Eq. (62) and by Eq. (67).** $\Delta\epsilon_\beta$ is the difference between the numerical solution for ϵ_β of the exact Eqs. (12), (14) and the approximate solutions for ϵ_β , Eq. (62) and (67), as a function of β at $W = 40$ for a $K = 2$ Cayley tree.

Surprisingly, for the Cauchy distribution Eq. (64) gives incredibly high accuracy for the localization transition point which is known exactly from Ref. [22]:

$$(4/\pi) K \ln[W_c/2] + 4 K^2/(3W_c) = W_c/2. \quad (69)$$

Numerical solution for this equation for $K = 2$ and $K = 3$ gives $W_c/2 = 4.36223$ and $W_c/2 = 9.09131$, respectively. The localization transition point can be also found from the equation [22]:

$$\epsilon_{\beta=1/2}(W) = 1/K. \quad (70)$$

Solving Eq. (70) with ϵ_β from Eq. (64) we found the following numbers: $W_c/2 = 4.36225$ for $K = 2$ and $W_c/2 = 9.09129$ for $K = 3$. This extra-ordinary accuracy seems to indicate on the accuracy of the approximation, Eq. (64), as high as $(W^4 \ln W)^{-1}$.

For the box probability distribution Eq. (70) with the approximate ϵ_β from Eq. (62) gives $W_c = 18.51$ which is close to the value $W_c = 18.17$ found numerically from the exact ϵ_β (see also [27, 30]). However, it is not so spectacularly close to the exact value as for the Cauchy distribution.

5 Statistics of Green's functions $G_{1,r}$ at large r

Given the moments, Eq. (3), one may find at large r the distribution function $P(y = \ln |G|)$ by evaluating the Mellin transform in the saddle-point approximation [25]. The distribution appears to have a very special form of the *large deviation ansatz*:

$$P(y = \ln |G|) \sim e^{r \ln K f(-\frac{2y}{r \ln K})}, \quad (71)$$

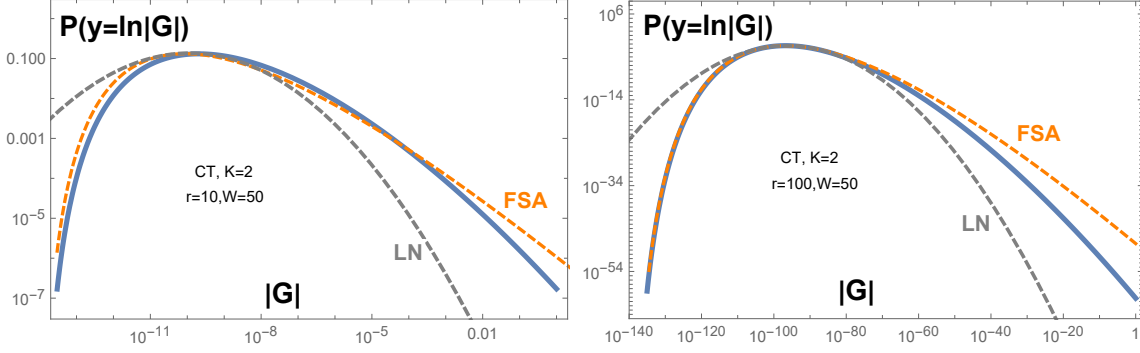


Figure 4: (Color online) **Comparison of PDF of $y = \ln |G|$ on the $K = 2$ Cayley tree** for the large- W approximation, Eq. (62) (solid blue line); the Poisson distribution in FSA, Eq. (2) (orange dashed line), and the log-normal (Gaussian in $\ln |G|$) distribution emerging from the Central Limit Theorem in FSA (gray dashed line) for two distances $r = 10$ (Left panel) and $r = 100$ (Right panel) at $W = 50$. The region $G_{typ} < |G| < 1$ of the solid blue curve corresponds to $0 < \beta < 1/2$, while the region $|G| < G_{typ}$ corresponds to the analytical continuation of ϵ_β to $\beta < 0$. The log-log derivative $d \ln P(y)/dy = -1$ at $|G| = 1$ which smoothly matches the tail $P(x = |G|) \sim G^{-2}$ at this point. The Poisson distribution emerging in FSA approximation at a finite r overestimates the probability of large deviations $|G| > G_{typ}$ from the typical value G_{typ} and the error increases with increasing the distance r . In contrast, in the region $|G| < G_{typ}$ the Poisson distribution becomes more accurate as r increases. The log-normal distribution is valid at small and moderate deviations from the typical value where all three distributions nearly coincide.

where the function $F(g)$ is given by the Legendre transform of $\ln \epsilon_\beta / \ln K$:

$$f(g) = \frac{\ln \epsilon_{\beta(g)}}{\ln K} + g \beta(g) \quad (72)$$

$$g = -\frac{1}{\ln K} \partial_\beta [\ln \epsilon_\beta] |_{\beta=\beta(g)}. \quad (73)$$

Eqs. (71), (72) are valid at large r at any disorder which is encoded into the form of β -dependence of ϵ_β . At small disorder $W/2 \lesssim 1$ important is the renormalization $\mathcal{F}(\epsilon)$ of on-site energy distribution $F(\epsilon)$ in Eq. (51) whereas at large disorder $W/2 \gg 1$ the deviation from FSA result, Eq. (2), is due to resonances which role is *overestimated* in FSA.

In Fig. 4 we compare: (i) $P(y = \ln |G|)$ for the large- W approximation (which is indistinguishable from the exact result at $W = 50$); (ii) Eq. (62), for the Poisson distribution, Eq. (2), resulting from FSA at the box distribution of on-site energies; and (iii) for the log-normal (Gaussian in $\ln |G|$) distribution which emerges from the Poisson distribution in the large r limit. We consider modestly strong disorder $W = 50$ and $r = 10, 100$.

Fig. 4 demonstrates the main physical result of this paper: FSA fails to describe large deviations $|G| \gg G_{typ}$ from the typical value G_{typ} , whereas the region $|G| \lesssim G_{typ}$ it describes quite well. As a matter of fact FSA *overestimates* the role of resonances which enhance $|G_{1,r}|$ at large distances r . The reason is that FSA, Eq. (1), involves the *on-site energies* ϵ_p along the shortest path rather than the exact eigenvalues E_p which emerge due to interference of the 'detour'/return paths of the length larger than r . Since those paths pass more than one time through the same sites, their amplitudes and the true eigenvalues are not statistically

independent. To take account of this important point, one should have considered in Eq. (1) the product of exact one-point Green's functions which take into account the real parts of self energies. The large- W approximations developed in this paper fix this drawback in an efficient way. It takes into account the fact that if at some point p of the path the one-point Green's function is large due to resonance $E_p \approx E$, it results in a large self energy for the Green's function on the next point $p + 1$ of the path. Thus the next Green's function must be small which compensates the large value of the preceding Green's function in the product. This mechanism of correlation [26] effectively diminishes the role of resonances and leads to a smaller probability of having the large value of $|G_{1,r}|$, as the Fig. 4 shows. This effect is more pronounced for long paths where the 'naive' resonances $\varepsilon_p = E$ appear in numbers $n_{\text{res}} \sim r$ proportional to the length. After the compensation, at most *one* resonance (out of n_{res}) may make contribution to the product if it occurs at the last point of the path. One can easily see this enhancement of the error of FSA as r increases comparing right and left panels of Fig. 4 and also on Fig. 1.

6 Conclusion

Our goal was to investigate the applicability of the forward scattering approximation (FSA) and to evaluate the probability distribution function of the Green's function for the Anderson localization model on sparse graphs at large disorder. Such graphs represent the Hilbert space of interacting quantum systems and FSA is often suggested as the simplest tool to approach the problem of Many Body Localization (MBL). The Hilbert space of the realistic models of MBL include graphs like a hypercube lattice of Quantum Ising model and Quantum Random Energy model or its cross-section of XXZ Heisenberg chain. Such graphs have numerous loops and thus many shortest-length trajectories with correlated amplitudes that interfere and make FSA rather complicated. However, even in the absence of such complication, on the Cayley tree, the applicability of FSA has severe limitations.

In this paper we have shown that FSA on the Cayley tree is not applicable in the limit of large distances r between points in the two-point Green's function, however large (but fixed) disorder strength is. It strongly overestimates the probability of large deviations $|G_r| > G_{\text{typ}}$ from the typical value of Green's functions due to ignoring the correlated character of resonances along the path connecting two point in a Green's function. The corresponding error increases with increasing the length of the path and in order to suppress it an unrealistically large disorder strength is required.

To arrive at this result, we computed the r -dependence of the moments of the real Green's function, relating them to the largest eigenvalue ε_β of the linearized transfer-matrix equation on a tree. This result, Eq. (3), is obtained by rigorous calculations in the framework of the Efetov's super-symmetry approach and it is valid at an arbitrary disorder strength. For strong disorder we derived very accurate large-disorder approximations, Eqs. (62), (63), (64), for ε_β and checked its accuracy against a high-precision numerical solutions of the Abou-Chacra-Thouless-Anderson equations for the box distributed on-site disorder and by a comparison to exact solution of the problem for the Cauchy distribution.

These results are encouraging to push forward the research on the distribution of Green's functions on the simplest realistic graphs emerging in the most popular models of MBL. The solution of this problem (to begin with the case of large disorder) would allow one to

construct an equivalent random-matrix model of the Rosenzweig-Porter type [24, 25, 31] which is amendable to a number of approximate methods of the mean-field type.

Acknowledgements

We are grateful to B. L. Altshuler, M. V. Feigelman and S. Raghu for insightful discussions.

Funding information The work of P.A.N. was supported in part by the US Department of Energy, Office of Basic Energy Sciences, Division of Materials Sciences and Engineering, under contract number DE-AC02-76SF00515. V. E. K. acknowledges the Google Quantum Research Award “Ergodicity breaking in Quantum Many-Body Systems” and Abdus Salam ICTP for support during this work. I. M. K. acknowledges the support of the Russian Science Foundation (Grant No. 21-12-00409). A. K. was supported by the Russian Science Foundation (Project No. 20-12-00224).

References

- [1] P. W. Anderson, Absence of diffusion in certain random lattices, Phys. Rev. **109**, 1492 (1958), doi:10.1103/PhysRev.109.1492.
- [2] J. Z. Imbrie, V. Ros and A. Scardicchio, Local integrals of motion in many-body localized systems, Annalen der Physik **529**, 1600278 (2017), doi:10.1002/andp.201600278.
- [3] V. Ros, M. Mueller and A. Scardicchio, Integrals of motion in the many-body localized phase, Nucl. Phys. B **891**, 420 (2015), doi:10.1016/j.nuclphysb.2014.12.014.
- [4] F. Pietracaprina, V. Ros and A. Scardicchio, Forward approximation as a mean-field approximation for the Anderson and many-body localization transitions, Phys. Rev. B **93**, 054201 (2016), doi:10.1103/PhysRevB.93.054201.
- [5] M. Tarzia, Many-body localization transition in Hilbert space, Phys. Rev. B **102**, 014208 (2020), doi:10.1103/PhysRevB.102.014208.
- [6] J. A. Kjäll, J. H. Bardarson and F. Pollmann, Many-body localization in a disordered quantum Ising chain, Phys. Rev. Lett. **113**, 107204 (2014), doi:10.1103/PhysRevLett.113.107204.
- [7] J. Z. Imbrie, On many-body localization for quantum spin chains, J. Stat. Phys. **163**, 998 (2016), doi:10.1007/s10955-016-1508-x.
- [8] D. A. Abanin and Z. Papić, Recent progress in many-body localization, Annalen der Physik **529**(7), 1700169 (2017), doi:https://doi.org/10.1002/andp.201700169, https://onlinelibrary.wiley.com/doi/pdf/10.1002/andp.201700169.
- [9] J. Z. Imbrie, V. Ros and A. Scardicchio, Local integrals of motion in many-body localized systems, Annalen der Physik **529**(7), 1600278 (2017), doi:https://doi.org/10.1002/andp.201600278, https://onlinelibrary.wiley.com/doi/pdf/10.1002/andp.201600278.

- [10] B. Derrida, Random-energy model: An exactly solvable model of disordered systems, Phys. Rev. B **24**, 2613 (1981), doi:10.1103/PhysRevB.24.2613.
- [11] Y. Y. Goldschmidt, Solvable model of the quantum spin glass in a transverse field, Phys. Rev. B **41**, 4858 (1990), doi:10.1103/PhysRevB.41.4858.
- [12] C. Manai and S. Warzel, Generalized random energy models in a transversal magnetic field: Free energy and phase diagrams, URL <https://arxiv.org/abs/2007.03290> (2020), 2007.03290.
- [13] D. Basko, I. L. Aleiner and B. L. Altshuler, Metal-insulator transition in a weakly interacting many-electron system with localized single-particle states, Ann. Phys. (N. Y). **321**(5), 1126 (2006), doi:10.1016/j.aop.2005.11.014.
- [14] A. Pal and D. A. Huse, Many-body localization phase transition, Phys. Rev. B **82**, 174411 (2010), doi:10.1103/PhysRevB.82.174411.
- [15] V. Oganesyan and D. A. Huse, Localization of interacting fermions at high temperature, Phys. Rev. B **75**, 155111 (2007), doi:10.1103/PhysRevB.75.155111.
- [16] D. J. Luitz, N. Laflorencie and F. Alet, Many-body localization edge in the random-field Heisenberg chain, Phys. Rev. B **91**, 081103 (2015), doi:10.1103/PhysRevB.91.081103.
- [17] D. J. Luitz and Y. B. Lev, The ergodic side of the many-body localization transition, Annalen der Physik **529**(7), 1600350 (2017), doi:<https://doi.org/10.1002/andp.201600350>, <https://onlinelibrary.wiley.com/doi/pdf/10.1002/andp.201600350>.
- [18] F. Alet and N. Laflorencie, Many-body localization: An introduction and selected topics, Comptes Rendus Physique **19**(6), 498 (2018), doi:<https://doi.org/10.1016/j.crhy.2018.03.003>, Quantum simulation / Simulation quantique.
- [19] D. A. Abanin, E. Altman, I. Bloch and M. Serbyn, Colloquium: Many-body localization, thermalization, and entanglement, Rev. Mod. Phys. **91**, 021001 (2019), doi:10.1103/RevModPhys.91.021001.
- [20] V. L. Nguyen, B. Z. Spivak and B. I. Shklovskii, Tunnel hopping in disordered systems, Zh. Eksp. Teor. Fiz. **89**, 1770 (1985).
- [21] K. Efetov, Supersymmetry in disorder and chaos, Cambridge University Press, doi:10.1017/CBO9780511573057 (1996).
- [22] R. Abou-Chacra, D. J. Thouless and P. W. Anderson, A selfconsistent theory of localization, Journal of Physics C: Solid State Physics **6**(10), 1734 (1973), doi:10.1088/0022-3719/6/10/009.
- [23] K. S. Tikhonov and A. D. Mirlin, Fractality of wave functions on a Cayley tree: Difference between tree and locally treelike graph without boundary, Phys. Rev. B **94**, 184203 (2016), doi:10.1103/PhysRevB.94.184203.

- [24] V. E. Kravtsov, I. M. Khaymovich, B. L. Altshuler and L. B. Ioffe, Localization transition on the random regular graph as an unstable tricritical point in a log-normal Rosenzweig-Porter random matrix ensemble, URL <https://arxiv.org/abs/2002.02979> (2020), 2002.02979.
- [25] I. M. Khaymovich and V. E. Kravtsov, Dynamical phases in a “multifractal” Rosenzweig-Porter model, URL <https://arxiv.org/abs/2106.01965> (2021), 2106.01965.
- [26] V. E. Kravtsov, B. L. Altshuler and L. B. Ioffe, Non-ergodic delocalized phase in Anderson model on Bethe lattice and regular graph, *Annals of Physics* **389**, 148 (2018), doi:10.1016/j.aop.2017.12.009.
- [27] G. Parisi, S. Pascazio, F. Pietracaprina, V. Ros and A. Scardicchio, Anderson transition on the Bethe lattice: an approach with real energies, *Journal of Physics A: Mathematical and Theoretical* **53**(1), 014003 (2019), doi:10.1088/1751-8121/ab56e8.
- [28] A. D. Mirlin and Y. V. Fyodorov, Localization transition in the Anderson model on the Bethe lattice: spontaneous symmetry breaking and correlation functions, *Nuclear Physics B* **366**(3), 507 (1991), doi:10.1016/0550-3213(91)90028-V.
- [29] M. R. Zirnbauer, Localization transition on the Bethe lattice, *Phys. Rev. B* **34**, 6394 (1986), doi:10.1103/PhysRevB.34.6394.
- [30] K. S. Tikhonov and A. D. Mirlin, Critical behavior at the localization transition on random regular graphs, *Phys. Rev. B* **99**, 214202 (2019), doi:10.1103/PhysRevB.99.214202.
- [31] I. M. Khaymovich, V. E. Kravtsov, B. L. Altshuler and L. B. Ioffe, Fragile ergodic phases in logarithmically-normal Rosenzweig-Porter model, *Phys. Rev. Research* **2**, 043346 (2020), doi:10.1103/PhysRevResearch.2.043346.